



## Photopyroelectric Spectrum of $\text{MnO}_2$ Doped $\text{Bi}_2\text{O}_3$ - $\text{TiO}_2$ - $\text{ZnO}$ Ceramic Combination

Zahid Rizwan<sup>1</sup>, Azmi Zakaria<sup>2\*</sup>, W. Mahmood Mat Yunus<sup>2</sup>, Mansor Hashim<sup>2</sup>  
and Abdul Halim Shaari<sup>2</sup>

<sup>1</sup>National Textile University, Sheikhupura road, Faisalabad (37610), Pakistan

<sup>2</sup>Department of Physics, Faculty of Science, Universiti Putra Malaysia,  
43400 UPM, Serdang, Selangor, Malaysia

\*E-mail: azmizak@fsas.upm.edu.my

### ABSTRACT

Photopyroelectric spectroscopy is used to study the energy band-gap of the ceramic ( $\text{ZnO} + 0.25 \text{Bi}_2\text{O}_3 + 0.25 \text{TiO}_2 + x \text{MnO}_2$ ),  $x = 0 - 1.3$  mol%, sintered at isothermal temperature 1190 and 1270°C for 2 hours in air. The wavelength of incident light, modulated at 9 Hz, is kept in the range of 300 to 800 nm and the photopyroelectric spectrum with reference to the doping level is discussed. The energy band-gap is estimated from the plot  $(phv)^2$  vs  $hv$  and is 2.80 eV for the samples without  $\text{MnO}_2$  at both sintering temperatures. It decreases to 2.08 eV with a further increase of  $\text{MnO}_2$ . The phase constitution is determined by XRD analysis. Microstructure and compositional analysis of the selected areas are analyzed using SEM and EDX. The maximum relative density, 91.4 %, and the grain size, 47  $\mu\text{m}$ , were observed in this ceramics combination.

**Keywords:** Photopyroelectric, band gap, zinc oxide

### INTRODUCTION

A white polycrystalline solid material Zinc Oxide ( $\text{ZnO}$ ) crystallizes into a wurtzite structure. It is a n-type semiconductor material with a wide energy band-gap 3.2 eV (Gupta, 1990). It is widely used in the manufacturing of paints, rubber products, cosmetics, pharmaceuticals, floor covering, plastics, textiles, ointments, inks, soap, batteries, and also in electrical components such as piezoelectric transducers, phosphors, solar cell electrodes, blue laser diodes, gas sensors and varistors (Lin *et al.*, 1998; Look, 2001).

The exact role of many additives in the electronic structure of  $\text{ZnO}$  varistors is uncertain.  $\text{ZnO}$  based varistor is formed with small amounts of metal oxides such as  $\text{Bi}_2\text{O}_3$ ,  $\text{Co}_3\text{O}_4$ ,  $\text{Cr}_2\text{O}_3$ ,  $\text{MnO}$ ,  $\text{Sb}_2\text{O}_3$  and others. These additives are the main tools that are used to improve the non-linear response and the stability of  $\text{ZnO}$  varistor (Eda, 1989). It is necessary to get information of optical absorption of the ceramic  $\text{ZnO}$  doped with different metal oxides. This paper reports the use of photopyroelectric (PPE) spectrometer, a powerful non-radiative tool (Mandelis, 1984) to study optical properties and a discussion on the PPE spectroscopy of  $\text{ZnO}$  doped with  $x\text{MnO}_2$  in the presence of 0.25  $\text{Bi}_2\text{O}_3$ , 0.25  $\text{TiO}_2$ .

Received : 11 January 2008

Accepted : 8 April 2008

\* Corresponding Author

### MATERIALS AND METHODS

ZnO (99.9 % purity) was doped with 0.25 Bi<sub>2</sub>O<sub>3</sub>, 0.25 TiO<sub>2</sub>, and xMnO<sub>2</sub> where x = 0 - 1.3 mol%. Pre-sintered powders at 760°C in air for 2 hours were pressed at 800 kg cm<sup>-2</sup> to form disk shape samples. Disks were sintered at 1190 and 1270°C for 2 hours in air at the heating and cooling rate of 2.5°C min<sup>-1</sup>. The density was measured by geometrical method. The mirror like polished samples were thermally etched for the microstructure analysis. Average grain size was determined by the grain boundary-crossing method. The disks of each sample were ground to make a fine powder for the PPE spectroscopic and XRD analysis. The XRD data were analyzed by using X'Pert High Score software for the identification of the crystalline phases. The measurement of PPE signal amplitude using the PPE spectrometer system to produce a PPE spectrum has been described elsewhere (Mandelis, 1984). In the present system, light beam was a 1 kW Xenon arc lamp that was kept in the range of 300 to 800 nm, mechanically chopped at 9 Hz, and scanned at 2 nm step size. The true PPE spectrum of the sample was obtained by normalizing PPE spectrum of sample with that of carbon black. Prior the PPE measurement, fine powder sample was ground in deionised water and a few drops of each mixture were dropped on 1.5 cm<sup>2</sup> aluminium foil and dried in air to form a thin sample layer about 12 µm thick on foil. The foil was placed in contact with PPE transducer (Tam and Coufal, 1983) using a very thin-layer of silver conductive grease. In determining the energy band-gap ( $E_g$ ), it was assumed that the fundamental absorption edge of doped ZnO is due to the direct allowed transition. The optical absorption coefficient  $\beta$  varies with the excitation light energy  $h\nu$  (Toyoda *et al.*, 1985) and is given by the expression,  $(\beta h\nu)^2 = C (h\nu - E_g)$  near the band gap, where  $h\nu$  is the photon energy,  $C$  is the constant independent of photon energy, and  $E_g$  is the direct allowed energy band-gap. The PPE signal intensity  $\rho$  is directly proportional to  $\beta$ , hence  $(\rho h\nu)^2$  is related to  $h\nu$  linearly. From the plot of  $(\rho h\nu)^2$  versus  $h\nu$ ,  $E_g$  is obtained by extrapolating the linear fitted region that crosses photon energy axis.

### RESULTS AND DISCUSSION

The XRD analysis, *Fig. 1*, of the ceramic shows that the major phase is hexagonal ZnO and the secondary phase is Bi<sub>4</sub>Ti<sub>3</sub>O<sub>12</sub> (ref. code 00-12-0213) developed in all samples at all doping levels and temperatures. Few peaks of Bi<sub>2</sub>O<sub>3</sub> (ref. code 00-018-0244), Mn<sub>2</sub>TiO<sub>4</sub> (ref. code 00-016-0241) were also observed in the pattern. Relative density increases from 88.7, 89.3% to 91.4, 90.6% with the increased of MnO<sub>2</sub> for 1190 and 1270 °C sintering temperatures, respectively, *Fig. 2*. It is slightly higher at lower sintering temperature. Grain size increased from 22.5, 24.8 to 46.3, 47.1 µm with the increase of MnO<sub>2</sub> for the sintering temperature 1190, 1270 °C, respectively, as depicted in *Fig. 3*. This indicates that the MnO<sub>2</sub> acts as a grain enhancer even in the presence of the other grain enhancers 0.25 Bi<sub>2</sub>O<sub>3</sub> and 0.25 TiO<sub>2</sub> which are present in the ceramic.

From SEM and EDX, *Fig. 5*, it shows that Bi<sub>2</sub>O<sub>3</sub> is segregated at grain boundaries as well as at triple point junctions. Some patches of the Zn, Ti, Mn additives were found on the grain surface of the grains. These are due to the in-homogeneous mixture of the ceramics. The energy band-gap ( $E_g$ ) of the ceramics is reduced from 3.2 eV (pure ZnO) to 2.80 ± 0.01 eV at the 0 mol% of MnO<sub>2</sub> for 1190 and 1270°C sintering temperatures, *Fig. 4*. The reduction of 0.40 ± 0.01 eV is due to the interface states produced by the combined effect of Bi<sub>2</sub>O<sub>3</sub> and TiO<sub>2</sub> additives at the two sintering temperatures. The energy band-gap is drastically decreased down to 2.24, 2.22 eV for sintering temperatures

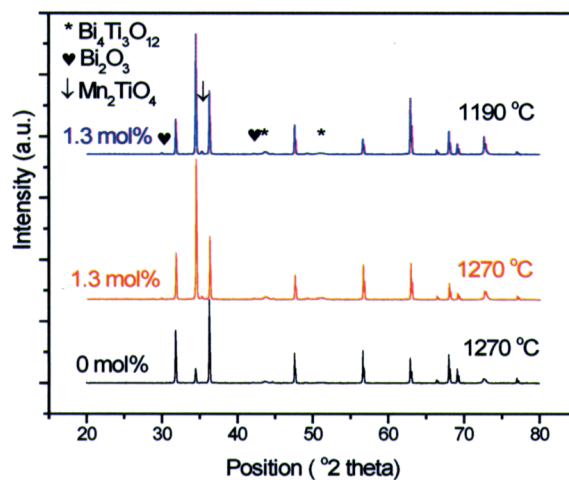


Fig. 1: XRD pattern at different doping level of  $\text{MnO}_2$

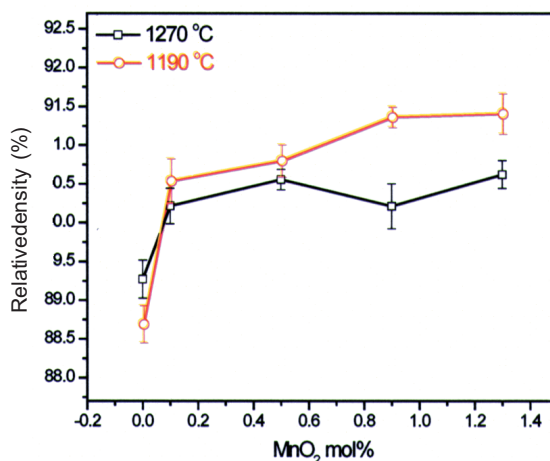


Fig. 2: Variation of density with  $\text{MnO}_2$

1190, 1270 °C, respectively, at 0.1 mol% of  $\text{MnO}_2$ . This rapid decrease is about 0.58 eV which is due to the growth of interface states in the grain interior and also in the grain boundaries. With further amount of  $\text{MnO}_2$  addition into the ceramic,  $E_g$  is found continuously decreasing down to 2.08 eV at 1.3 mol% of  $\text{MnO}_2$  at both sintering temperatures. This small decrease, about 0.14 eV, is due to the growth of interface states with the addition of  $\text{MnO}_2$  (Toyoda and Shimamoto, 1998). The overall value of  $E_g$  is slightly lower at the higher sintering temperature at all doping levels. This indicates that the increase in the sintering temperature is not effective at decreasing the value of  $E_g$ . It is observed that the decrease in the  $E_g$  due to the combined effect of the 0.25  $\text{Bi}_2\text{O}_3$  and 0.25  $\text{TiO}_2$  additives at both sintering temperatures is about 0.40 eV but the decrease in

$E_g$  is about 0.58 eV only at 0.1 mol%  $MnO_2$ . Ionic radius of Mn ion (0.53 Å) is smaller than the ionic radius of Zn (0.74 Å) (Yoshikazu *et al.*, 2002; Dow and Redfield, 1972; Urbach, 1953) so Mn ions substitutes the Zn ions and contributes to further increase of interface states hence further decrease of  $E_g$ .

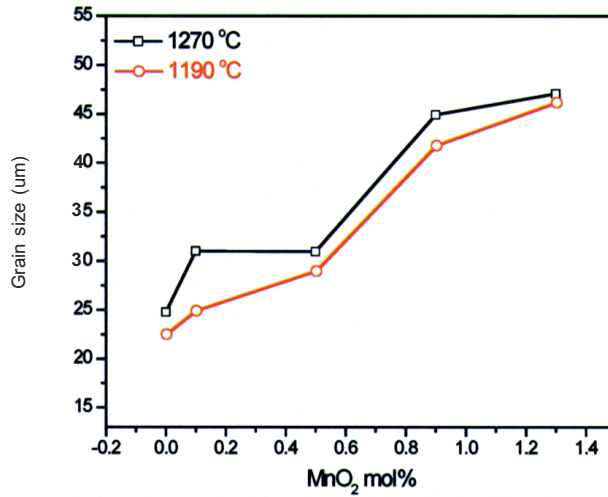


Fig. 3: Variation of grain size with  $MnO_2$

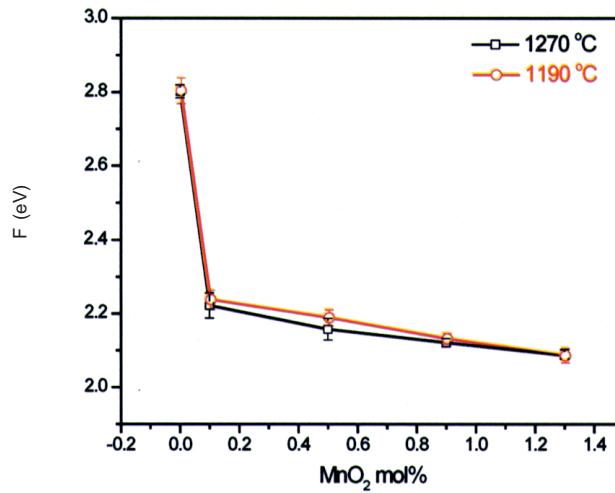


Fig. 4: Dependence of  $E_g$  on  $MnO_2$

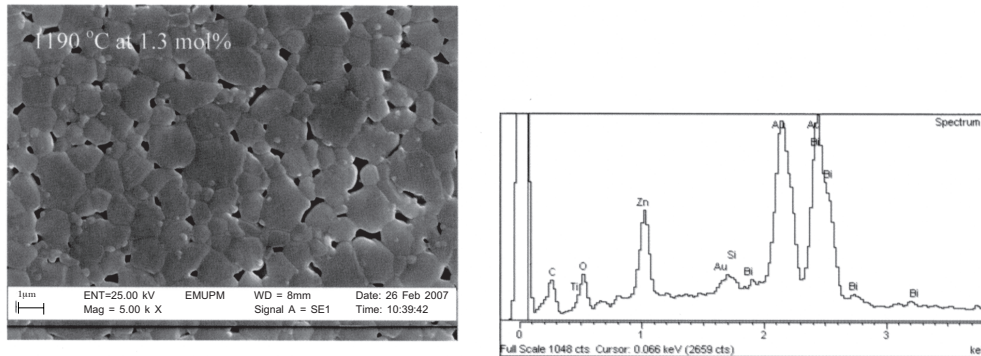


Fig. 5: SEM micrograph for 1.3 mol% and EDX spectrum at the grain boundary for 0.1 mol%  $\text{MnO}_2$  at 1190 °C sintering temperature

## CONCLUSIONS

Spectroscopic results are discussed with the doping of  $\text{MnO}_2$  and found that the  $\text{MnO}_2$  acts as a grain enhancer. Both  $\text{Bi}_2\text{O}_3$  and  $\text{TiO}_2$  reduce the energy band-gap but  $\text{MnO}_2$  does contribute more prominently.

## ACKNOWLEDGEMENTS

Thanks to MOSTI for the financial assistance (Grant FRGS No. 01-01-07-139FR) for this research.

## REFERENCES

- DOW, J.D. and REDFIELD, D. (1972). Towards a unified theory of Urbach's rule and exponential absorption edge. *Phys. Rev.*, *B5*, 594.
- EDA, K. (1989). Zinc oxide varistors. *IEEE Elect. Insul. Mag.*, *5*, 28-41.
- GUPTA, T.K. (1990). Application of zinc oxide varistors. *J. Am. Ceram. Soc.*, *73*(7), 1817-40.
- LIN, H.M., TZENG, S.J., HSIAU, P.J. and TSAI, W.L. (1998). Electrode effects on gas sensing properties of nanocrystalline zinc oxide. *Nanostruct. Mater.*, *12*, 465- 77.
- LOOK, D.C. (2001). Recent advances in ZnO materials and devices. *Mat. Sci. Eng. B*, *80*, 383-87.
- MANDELIS, A. (1984). Frequency-domain photopyroelectric spectroscopy of condensed phases (PPES): A new, simple and powerful spectroscopic technique. *Chem. Phys. Lett.*, *108*, 388-92.
- TAM, A.C. and COUFAL, H. (1983). Photoacoustic generation and detection of 10-ns acoustic pulses in solids. *Appl. Phys. Lett.*, *42*, 33-5.
- TOYODA, T., NAKANISHI, H., ENDO, S., and IRIE, T. (1985). Fundamental absorption edge in semiconductor  $\text{CdInGaS}_4$  at high temperatures. *J. Phys. D Appl. Phys.*, *18*, 747-51.
- TOYODA, T. and SHIMAMOTO, S. (1998). Effect of  $\text{Bi}_2\text{O}_3$  impurities in ceramic ZnO on photoacoustic spectra and current-voltage spectra. *Jpn. J. Appl. Phys.*, *37*, 2827-31.



Zahid Rizwan, Azmi Zakaria, W. Mahmood Mat Yunus, Mansor Hashim and Abdul Halim Shaari

YOSHIKAZU, S., YASUHIRO, O., TOSHIO, K. and JUN, M. (2002). Evaluation of  $\text{Sb}_2\text{O}_3$ -doped ZnO varistors by photoacoustic spectroscopy. *Jpn. J. Appl. Phys.*, 41, 3379-82.

URBACH, F. (1953). The long-wavelength edge of photographic sensitivity end of the electronic absorption of solids. *Phys. Rev.*, 92, 1324.

